The Influence of Mn(II) and Aging Time in the Ferrihydrite to Goethite Transformation

Mariana Alvarez[1,*], Elsa H. Rueda[1], Carlos O. Paiva-Santos[2] and Elsa E. Sileo[3]

[1]*Departamento de Química, Universidad Nacional del Sur - Av. Alem 1253 -B8000CPB - Bahía Blanca, Argentina;* [2]*Instituto de Química, UNESP - R. Prof. Francisco Degni s/n, 14800-900 – Araraquara, SP - Brasil and* [3]*INQUIMAE, Dpto. de Química Inorgánica, Analítica y Química Física - Facultad de Ciencias Exactas y Naturales - Universidad de Buenos Aires - Pabellón II, Ciudad Universitaria - C1428EGA - Buenos Aires, Argentina*

Abstract: The ferrihydrite-goethite transformation in samples of pure- and Mn-ferrihydrite was investigated in order to elucidate the effect of Mn(II) in the aging process. Samples of pure- and Mn-ferrihydrites were aged for different times, and their structural changes were described on the basis of Rietveld structure refinements. A comparison of two series of samples with (A-series) and without Mn (F-series) shows *b*- enlargement and *a*- and *c*- shortening due to the presence of Mn during the complete aging process. However, with aging different trends are observed in both the series. In the samples synthesized without Mn(II) the variations in all the unit-cell constants are virtually negligible, whereas in the series with Mn(II) more significant changes are reflected by the enlargement of *a*- and *c*- and the shortening of the *b*. These results confirm that the dimensions of the lattice parameters depend not only on the substitution ratio but also on the aging history of the sample.

INTRODUCTION

Iron oxides and oxyhydroxides minerals are of great importance in the environment as well as in industry. Poorly crystalline Fe(III)-oxides (ferrihydrites) commonly exist in soils and sediments and are thermodynamically unstable. Ferrihydrites, with time, are transformed to more crystalline Fe(III) oxides [1]. This transformation proceeds through two competing mechanisms [2,3]. Goethite formation involves the dissolution of ferrihydrite and reprecipitation from solution whereas hematite forms by dehydration and atomic reordering of the solid ferrihydrite. Hematite formation is favored by conditions that depress the solubility of ferrihydrite, whereas the formation of goethite is favored when the solubility and dissolution rate of ferrihydrite increases.

Ferrihydrite with 2-(XRD) line and 6-line varieties are commonly obtained in laboratory experiments, although species with an intermediate numbers of reflections have been found in nature. The structural and genetic relationship between 2- and 6-line ferrihydrite is obscure. The results obtained by Schwertmann *et al.* [4] strongly suggest that the different ferrihydrites do not form a genetic series in which the six-line variety forms by the gradual ordering of a less crystalline precursor, because these forms of ferrihydrites precipitate under different conditions. On the other hand, Kukkadapu *et al*. [5] using a variety of techniques including X-ray diffraction (XRD), Mössbauer spectroscopy (MS) and transmission electron microscopy (TEM) demonstrated that 6-line ferrihydrite could form as the transformation product of 2-line ferrihydrite under various conditions. Recently, Michel *et al.* [6] presented results from synchrotron-based X-ray total scattering experiments, which indicate that both the short- and intermediate-range ordering in nanocrystalline ferrihydrite are essentially the same and independent of changes in particle size. These results represent an important step in quantifying the terms of the so-called 2- and 6-line forms and significantly advance on the understanding of the atomic arrangements in nanocrystalline ferrihydrite; this will lead to a better understanding its structure, reactivity, and other interesting properties.

The presence of foreign species of anions, cations and neutral molecules in the system can have two different effects on the transformation of ferrihydrite to other iron oxides [7-9]. They can either modify the kinetics of transformation by slowing the process, or change the composition and properties of the end product. Cations usually require mol ratios of 0.05-0.1 to influence the kinetics of the reaction products, whereas anions are often effective at lower concentrations [1]. In addition to the retardation effects, cations are often incorporated in the iron oxide structure. A detailed examination of the structure of the ferrihydrite/solution interface and the manner in which the metals are incorporated into the solid, is required to understand the effects of the different divalent and trivalent cations on the stability of ferrihydrite. However, the poorly ordered nature of ferrihydrite complicates this attempt. Nevertheless, the elucidation of the reaction mechanisms and an estimation of the associated transport and thermodynamic parameters are important for an accurate description of the fate of toxic metal pollutants in soils and aquatic ecosystems rich in iron oxides [10].

The transformation in samples of pure- and Mn-ferrihydrite to elucidate the effect of the presence of Mn(II) in the aging process was chosen because the actual pathway of the

*Address correspondence to this autor at the Departamento de Química, Universidad Nacional del Sur - Av. Alem 1253 -B8000CPB - Bahía Blanca, Argentina; Tel: +54-291-4595159; E-mail: alvarezm@pop3.criba.edu.ar

1874-4567/08

goethite-ferrihydrite transformation process is unclear and also can be affected by the presence of foreign cations. For this purpose several samples of pure- and Mn-ferrihydrites were aged for different times, and the structural changes of the obtained oxihydroxides were described by the Rietveld method using X-ray powder diffraction data [11].

MATERIALS AND METHODS

A set of five samples of ferrihydrites was synthesized by adding aqueous $Fe(NO_3)_3$ (25 mL, 0.53 M) to NaOH (87.5 mL, 2 M). The resultant precipitates were centrifuged, washed twice with double distilled water, and aged in Teflon bottles at 60 ºC in NaOH solutions (125 mL, 0.3 M) for 4, 8, 12, 16, 20 and 24 hours, respectively. Samples were labeled F_i (with $4 < i < 24$).

A series of Mn-ferrihydrites was obtained by a similar method, by the coprecipitation of a mixture of $Fe(NO_3)_3$ and $Mn(NO_3)_2$ 0.53 M solutions with NaOH 2 M. The molar ratio Mn/(Mn + Fe) was kept at 0.10. Aging times were 8, 12, 16, 20 and 24 hours.

The final solids were washed, dried and gently crushed. In order to remove the poorly crystalline compounds from the precipitates, half of each sample of the A-series was extracted in the dark with ammonium oxalate (0.2 M, pH 3.0) for 4 hours at room temperature [12]. The non-extracted and the extracted samples were identified as A_i and A'_i (with $8 < i < 24$), respectively.

The Mn and Fe contents of the solids were determined by atomic absorption spectrometry (AAS) in a GBC Model B-932 spectrometer. Chemical analyses were performed in duplicates by dissolving 20 mg samples, at 60-80 ºC, in 100 mL HCl 6 M.

X-ray diffraction patterns were recorded using a Siemens D5000 diffractometer, operated at 40 kV and 35 mA, in a Bragg-Brentano geometry and equipped with Cu$K\alpha$ radiation and a graphite monochromator. Data were collected in the $18.500^{\circ} \leq 2\theta \leq 132.000^{\circ}$ range, with a scanning step of 0.025°. Divergence scattered and receiving radiation slits were 1°, 1° and 0.2 mm respectively.

The structural refinement was conducted using the program package GSAS [13]. Peak profiles were fitted using the Thompson-Cox-Hastings pseudo-Voigt function [14] with the microstrain broadening description of Stephens [15]. Peaks asymmetry was corrected using the Finger function [16]. The crystallite sizes were obtained by adopting the anisotropic bidimensional model described in the GSAS manual. The crystallite size was then determined in the parallel direction (P_{paral}) and perpendicular direction (P_{perp}) to the anisotropic broadening (021) axis. Crystallite dimensions were calculated making allowances for the instrument broadening function that was previously modeled using NIST SRM 660 lanthanum hexaboride (LaB_6) standard.

RESULTS AND DISCUSSION

Table **1** shows the metal contents for samples belonging to the A-series measured before and after the ammonium oxalate treatment.

As can be seen, the Mn molar ratio in the unextracted samples remains essentially constant (~ 0.118 ± 0.003 mol mol^{-1}). This result agrees with an almost negligible Mn content in the supernatants after the solid separation, and indicates that Mn is completely adsorbed and/or incorporated to the oxide. In the extracted samples, x_{Mn} shows greater values indicating the dissolution of amorphous Fe oxides during the extraction process.

Table 1. Chemical Composition for Samples Belonging to the A-Series

Sample	x_{Fe} (Before O. E.)	x_{Mn} (Before O. E.)	x_{Fe} (After O. E.)	x_{Mn} (After O. E.)
A_8	0.885(1)	0.115(2)	0.870(3)	0.130(2)
A_{12}	0.884(1)	0.116(1)	0.864(2)	0.136(2)
A_{16}	0.880(2)	0.120(2)	0.871(2)	0.129(3)
A_{20}	0.881(3)	0.119(3)	0.865(1)	0.135(1)
A_{24}	0.879(2)	0.121(1)	0.867(2)	0.133(2)

O. E.: oxalate extraction.
x_{Mn}: Mn content, expressed as Mn/(Mn + Fe) mol mol^{-1}
x_{Fe}: Fe content, expressed as Fe/(Mn + Fe) mol mol^{-1}

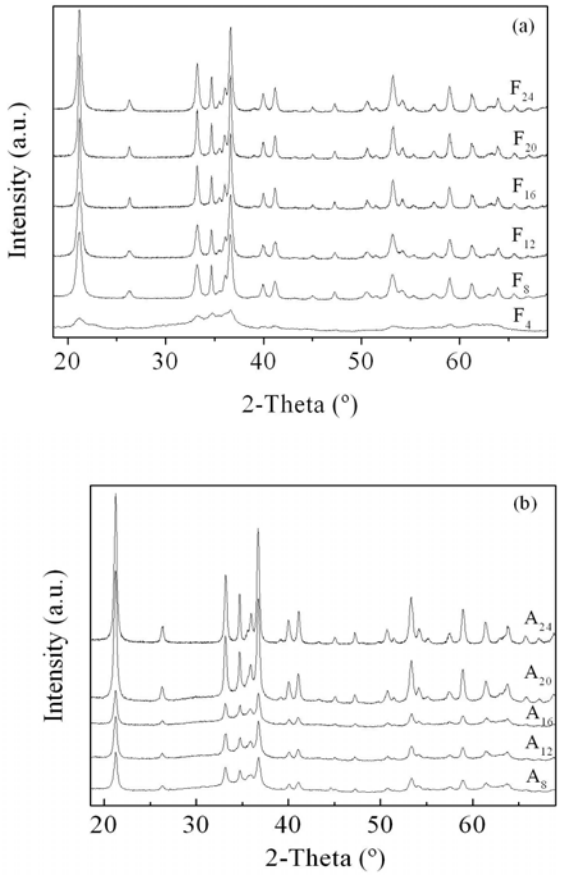

Fig. (1). XRD patterns: (**a**) F- series and (**b**) A-series.

The small changes observed in XRD peak positions of all samples (Fig. **1**) indicate changes in the unit cell parameters resulting from differences in aging times. Only sample F_4 shows a decrease of crystallinity in F-series. From F_8 to F_{24},

the XRD patterns show the presence of a well-crystallized goethite phase. Samples belonging to the A-series show a slower transformation to the goethite phase. Except for A_{24}, all samples in A-series display a lower degree of crystallinity than the corresponding pure samples. Only in the step $A_{20} \rightarrow A_{24}$ a well-crystallized goethite is formed. These results indicate that the presence of Mn(II) retards the ferrihydrite-goethite transformation by stabilizing ferrihydrite towards dissolution. However, this stabilization effect is not strong enough to promote the ferrihydrite-hematite transformation. Cornell and Giovanoli [8] also found that the rate of transformation of ferrihydrite in the presence of Mn(II) was slightly slower than that of the pure ferrihydrite.

The XRD patterns of samples of both series have been simulated using the Rietveld method. The values of the reliability factors that describe the quality of the fitting, Rwp, Rp, R_B and GofF were in the range 7.05–9.37%, 5.24-7.13%, 2.81–3.84% and 1.11–1.24, respectively. Because of the low crystallinity in the A-series, only cell parameters and crystallite sizes have been refined in samples A_8 to A_{24}.

Variations in lattice parameters obtained by Rietveld refinement of both series of samples are presented in Table **2** and a comparison of the unit-cell constants is presented in Fig. (**2**).

Table 2. Unit-Cell Constants and Crystallite Dimensions in the F- and A-Series

Sample	*a* (Å)	*b* (Å)	*c* (Å)	P_{paral}/P_{perp} [a] (Å)
F_8	4.6160(3)	9.9564(4)	3.0248(1)	837 / 169
F_{12}	4.6139(3)	9.9565(1)	3.0244(1)	721 / 197
F_{16}	4.6109(2)	9.9586(3)	3.0236(1)	749 / 377
F_{20}	4.6108(2)	9.9580(3)	3.0237(1)	768 / 361
F_{24}	4.6114(2)	9.9576(3)	3.0241(1)	617 / 448
A_8	4.5961(9)	9.9971(9)	3.0139(5)	527 / 279
A_{12}	4.5977(7)	9.9973(9)	3.0124(3)	318 / 326
A_{16}	4.5975(8)	9.9932(13)	3.0132(3)	294 / 316
A_{20}	4.5972(2)	9.9923(4)	3.0148(1)	414 / 326
A_{24}	4.5989(2)	9.9826(3)	3.0180(1)	972 / 351

[a]: P_{paral} and P_{perp} are the crystallite sizes parallel and perpendicular to the (021) axis, respectively.

The cell dimensions are markedly different in both the series. In the A-series, *a* and *c* are smaller than in the F-series, whereas the *b*-values are larger than those in the F-series. These results are consistent with preliminary data that confirm the *b*- enlargement and the *a*- and *c*- shortening of the unit-cell constants with Mn-substitution in the goethite structure [17-19].

Inside each series the parameters also change. The variations in pure goethite are small, with the *a*-parameter decreasing from F_8 to F_{20}, and slightly increasing in F_{24}. The variations in *b*- and *c*-values are almost negligible and vary non-monotonically In the A-series the *a*-dimension increases slightly from A_8 to A_{12}, but remains virtually constant up to A_{20} and increases in A_{24}. The changes in *b*- and *c*-values are more marked; *b*- decreases progressively with the aging period and *c*- decreases from A_8 to A_{12} and then shows an increment in A_{24}.These results confirm that the dimensions of the cell parameters depend not only on the substitution ratio but also on the aging history of the sample.

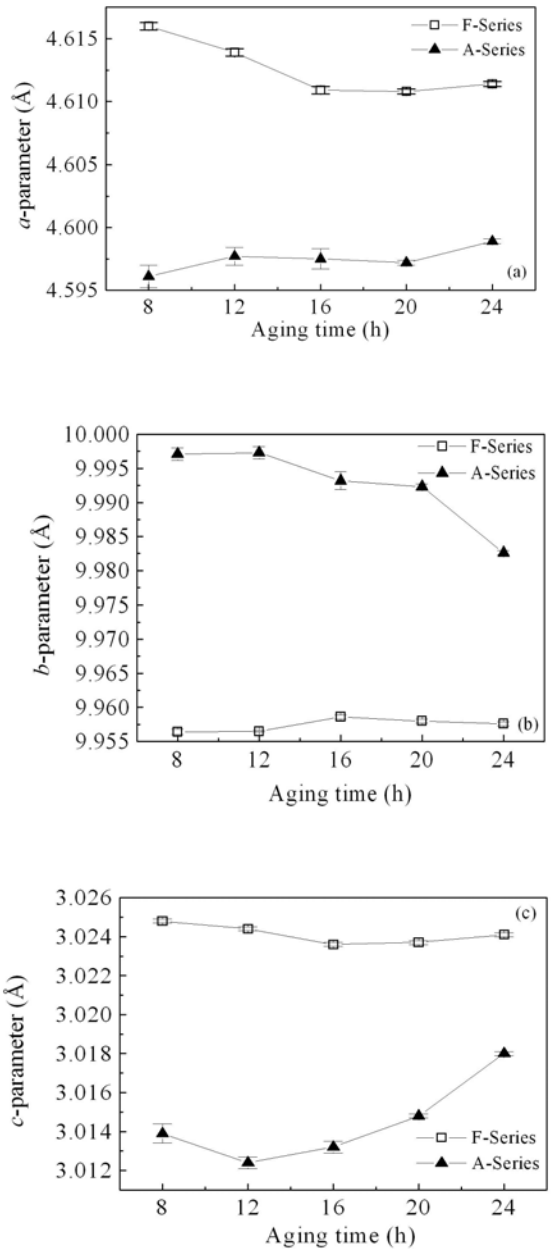

Fig. (2). (**a**) *a*-,(**b**) *b*-, and (**c**) *c*-lattice dimensions in the A- and F-series vs. aging time.

The crystallite sizes also change with the aging time. The values in the F-series (pure goethite) indicate that the size parallel to (021) decreases with the aging time and the dimension perpendicular to the (021) axis increases (from 837 to 617 Å and from 169 to 448 Å, respectively). In general, the Mn-goethites values are smaller than those of pure-

Table 3. Refined Atomic Positions for the Samples of the F-Series

Sample	Fe		O		OH		H	
	x	*y*	*x*	*y*	*x*	*y*	*x*	*y*
F_8	0.0470(2)	-0.1458(1)	-0.2931(7)	0.1982(3)	0.1961(6)	0.0527(3)	0.3906(26)	0.0822(22)
F_{12}	0.0485(2)	-0.1459(1)	-0.2923(7)	0.1991(3)	0.1969(1)	0.0519(4)	0.3753(26)	0.0993(22)
F_{16}	0.0494(2)	-0.1460(1)	-0.2956(8)	0.1997(3)	0.2029(8)	0.0511(3)	0.3760(48)	0.1034(31)
F_{20}	0.0489(2)	-0.1460(1)	-0.2909(8)	0.1988(4)	0.1980(7)	0.0529(3)	0.3868(21)	0.0892(27)
F_{24}	0.0482(2)	-0.1460(1)	-0.2905(7)	0.1997(3)	0.1997(3)	0.0517(3)	0.3858(21)	0.1052(44)

Table 4. Interatomic Distances (Å) for the Samples Belonging to the F-Series

Sample	Fe-O(a)	Fe-O(b)	Fe-OH(a)	Fe-OH(b)	E'	E	DC
F_8	1.947(4)	2×1.960(2)	2.092(3)	2×2.101(3)	2×3.0248(1)	2×3.304(1)	4×3.452(1)
F_{12}	1.944(5)	2×1.958(3)	2.086(4)	2×2.108(3)	2×3.0244(1)	2×3.306(1)	4×3.450(1)
F_{16}	1.932(4)	2×1.965(3)	2.085(3)	2×2.128(3)	2×3.0236(1)	2×3.307(2)	4×3.449(1)
F_{20}	1.951(4)	2×1.951(3)	2.097(3)	2×2.107(3)	2×3.0237(1)	2×2.308(2)	4×3.448(1)
F_{24}	1.942(3)	2×1.955(2)	2.085(3)	2×2.108(3)	2×3.0242(1)	2×3.308(2)	4×3.448(1)

goethites. The changes are not monotonic as in the F-series, and A_{24} presents a surprisingly higher value in P_{paral}. To clarify the simultaneous effect of Mn incorporation and aging time over the crystallite size, we consider that new techniques as high-resolution X-ray pair distribution function (PDF) measurements should be applied to give more accurate information about local, intermediate and long-range structure [20].

The refined atomic positions for the samples belonging to the F-series are presented in Table **3**.

The atomic distances Fe-OH, Fe-O and Fe-Fe in the goethite samples obtained in F-series, have been calculated and are presented in Table **4**.

The structure of goethite is based on a hexagonal close-packed array of anions (O^{2-}, OH^-) with half of the octahedral sites filled with Fe(III) cations. The $Fe(O,OH)_6$ octahedra are joined by an edge, through two OH^- groups, forming a double link. The double links form chains that run along the (001) direction [21,22]. The chains are joined one to another by O^{2-} ligands. This structure generates three different Fe-Fe distances. Into the link the two Fe ions joined by two OH^- determine the distance named E; into each chain, and in the *c*-direction, the Fe ions joined by one O^{2-} and one OH^- determine the distance named E´; and between chains the Fe ions joined by O^{2-} determine the distance named DC. These features are shown in Fig. (**3**).

As can be seen, E' depends on the Fe-OH(b) and Fe-O(b) distances and on the O(b)-Fe-OH(b) angle. Data in Table **4** allow a comparison between the structure of the less (F_8) and the more aged sample (F_{24}). From F_8 to F_{24}, the E' distance (coinciding with the *c*-parameter) decreases. The Fe-OH(b) slightly increases (from 2.101(3) to 2.108(3) Å), and Fe-O(b) decreases (from 1.960(2) to 1.955(2) Å); the O(b)-Fe-OH(b) angle does not change significantly. These variations indicate that the change in Fe-O(b) dominates the observed trend in the *c*-dimension.

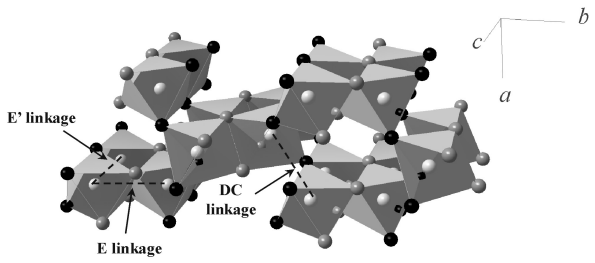

Fig. (3). Clinographic view of the goethite structure showing the three different Fe-Fe linkages.

Fe-OH(a) and Fe-OH(b) distances and angle OH(a)-Fe-OH(b) influence the variation on E distance that increases with the aging time. As Fe-OH(b) increases from 2.101(3) Å to 2.108(3), Fe-OH(a) varies from 2.092(3) to 2.085(3), and angle OH(b)-Fe-OH(a) enlarges from 76.04(2) to 76.26(2)º, the slight increment in E distance (from 3.304(1) to 3.308(2) Å) is principally determined by the Fe-OH(a) change.

Both the Fe-O distances and the Fe-O-Fe angle determine the third Me-Me distance, DC. The average distance Fe-O changes from 1.956 to 1.951 Å, and the corresponding angle increases from 124.12(2) to 124.48(2)º. Consequently, the decrease in DC distance is attributed to the decrease of both Fe-O distances.

In general, these changes explain the variations of all the unit-cell constants due to changes in Fe-O or Fe-OH distances. The enlargement of the *b*- and the decrease of the *a*-parameter in the F-series give rise to a decrease of the unit-cell volume, leading to a more compact structure during the ferrihydrite-goethite transformation process.

CONCLUSIONS

A comparison of two series of samples with and without Mn involving the transformation of ferrihydrite to goethite shows a *b*- enlargement and *a*- and *c*- shortening due to the presence of Mn during the complete aging process.

For each of the two series, different trend of the unit-cell constants behaviour is observed as a function of the aging time. In the F-series the variations of all the cell parameters are practically negligible, except for a general decrease observed for *a*. In contrast, in the A-series more significant changes are observed in the enlargement of *a* and *c* and the shortening of *b* from A_8 to A_{24}. These results confirm that the dimensions of lattice parameters depend not only on the Mn/Fe substitution but also on the aging history of the sample.

The crystallite sizes also change. The values in the F-series (pure goethite) indicate that the dimension perpendicular and parallel to the (021) axis decrease and increase respectively with aging. In general the values in Mn-goethites are smaller than in pure-goethites. Only the more aged Mn-goethite presents a higher value in p_{perp}.

ACKNOWLEDGEMENTS

This research was partially supported by grants UBA-CYT X-800, PICT -2005 32469 and by Secretaría de Ciencia y Tecnología (UNS).

REFERENCES

[1] Cornell, R.M.; Schwertmann,U. The iron oxides. Structure, Properties, Reaction,Occurrence and Uses. VCH, Weinheim, Germany, **1996**.

[2] Schwertmann, U.; Murad, E. Effect of pH on the formation of goethite and hematite from ferrihydrite. *Clays Clay Miner*., **1983**, *31*, 277-284.

[3] Johnston, J.H.; Lewis, D.G. A study of the initially-formed hydrolysis species and intermediate polymers and their role in determining the product iron oxides formed in the weathering of iron. Long, G.J.; Stevens, J.G. Eds.; Industrial applications of the Mössbauer effect: Plenum Press, New York, **1986**; pp. 565-583.

[4] Schwertmann, U.; Friedl, J.; Stanjek, H. From Fe(III) Ions to Ferrihydrite and then to Hematite. *J. Colloid Interface Sci.*, **1999**, *209*, 215-223.

[5] Kukkadapu, R.K.; Zachara, J.M.; Fredrikson, J.K.; Smith, S.C.; Dohnalkova, A.C.; Russell, C.K. Transformation of 2-line ferrihydrite to 6-line ferrihydrite under oxic and anoxic conditions. *Am. Miner*., **2003**, *88*, 1903-1914.

[6] Michel, F.M.; Ehm, L.; Liu, G.; Han, W. Q.; Antao, S. M.; Chupas, P. J.; Lee, P. L.; Knorr, K.; Eulert, H.; Kim, J.; Grey, C. P.; Celestian, A. J.; Gillow, J.; Schoonen, M. A. A.; Strongin, D. R.; Parise, J. B. Similarities in 2- and 6-Line Ferrihydrite Based on Pair Distribution Function Analysis of X-ray Total Scattering. *Chem. Mater.*, **2007**, *19*, 1489-1496.

[7] Lewis, D.G.; Schwertmann, U. The influence of A1 on iron oxides. Part III. Preparation of A1-goethites in KOH. *Clay Miner*., **1979**, *14*, 115-126.

[8] Cornell, R.M.; Giovanoli, R. Effect of manganese on the transformation of ferrihydrite into goethite and jacobsite in alkaline media. *Clays Clay Miner*., **1987**, *35*, 11-20.

[9] Cornell, R.M.; Giovanoli, R. The influence of copper on the transformation of ferrihydrite ($5Fe_2O_3$•$9H_2O$) into crystalline products in alkaline media. *Polyhedron*, **1988**, *7*, 385-391.

[10] Triverdi, P.; Dyer, J. A.; Sparks, D. L.; Pandya, K. Mechanistic and thermodynamic interpretations of zinc sorption onto ferrihydrite. *J. Colloid Interface Sci.*, **2004**, *270*, 77-85.

[11] Rietveld, H.M. A profile refinement method for nuclear and magnetic structures. *J. Appl. Crystallogr*., **1969**, *2*, 65-71.

[12] Schwertmann, U. Differenzierung der Eisenoxide des Bodens durch Extraktion mit Ammoniumoxalat-Lösung. *Z.P flanzenernähr Düng Bodenkd*., **1964**, *105*, 194-202.

[13] Larson, A.C.; Von Dreele, R.B. *General Structure Analysis System (GSAS)*. Los Alamos National Laboratory Report LAUR, **2004**, 86.

[14] Thompson, P.; Cox, D.E.; Hastings, J.B. Rietveld refinement of Debye-Scherrer synchrotron X-ray data from Al2O3. *J. Appl. Crystallogr.*, **1987**, *20*, 79-83.

[15] Stephens, P.W. Phenomenological model of anisotropic peak broadening in powder diffraction. *J. Appl. Crystallogr*., **1999**, *32*, 281-289.

[16] Finger, L.W.; Cox, D.E.; Jephcoat, A.P. A correction for powder diffraction peak asymmetry due to axial divergence. *J. Appl. Crystallogr*., **1994**, *27*, 892-900.

[17] Stiers, W.; Schwertmann, U. Evidence for manganese substitution in synthetic goethite. *Geochim. Cosmochim. Acta*, **1985**, *49*, 1909-1911.

[18] Sileo, E.E.; Alvarez, M.; Rueda, E.H. Structural studies on the manganese for iron substitution in the synthetic goethite-jacobsite system. *Int. J. Inorg. Mater*., **2001**, *3*, 271.

[19] Alvarez, M.; Sileo, E.E.; Rueda, E.H. Effect of Mn(II) incorporation on the transformation of ferrihydrite to goethite. *Chem. Geol*., **2005**, *216*, 89.

[20] Billinge, S.J.L.; Kanatzidis, M.G. Beyond crystallography: the study of disorder, nanocrystallinity and crystallographically challenged materials with pair distribution functions. *Chem. Commun*., **2004**, 749-760.

[21] Megaw, H.D. *Crystal Structures: A Working Approach*. W.B. Saunders Company: Philadelphia, **1973**.

[22] Cornell, R.M.; Mann, S.; Skarnoulis, A.J. *J. Chem. Soc. Faraday Trans. I*., **1983**, *79*, 1679.

Received: October 31, 2007 Revised: June 30, 2008 Accepted: September 11, 2008